

# Visualization of Strain-Induced Structural Rearrangements in Amorphous Poly(ethylene terephthalate)<sup>1</sup>

A. L. Volynskii, T. E. Grokhovskaya, A. I. Kulebyakina, A. V. Bol'shakova,  
L. M. Yarysheva, D. A. Panchuk, A. V. Efimov, and N. F. Bakeev

Faculty of Chemistry, Moscow State University,  
Leninskie gory, Moscow, 119992 Russia  
e-mail: volynskii@mail.ru

Received May 23, 2005;

Revised Manuscript Received December 9, 2005

**Abstract**—A direct microscopic observation procedure is applied to study the deformation of amorphous PET decorated with a thin metal layer when stretching is performed at different draw rates and at temperatures below and above the glass transition temperature  $T_g$ . Analysis of the formed microrelief allows stress fields responsible for the deformation of the polymer to be visualized and characterized. When tensile drawing is performed at temperatures above  $T_g$ , inhomogeneity of stress fields increases with the increasing draw rate; at high draw rates, the stress-induced crystallization of PET takes place. In the case of drawing the polymer at temperatures below  $T_g$ , direct microscopic observations make it possible to visualize the development of shear bands that appear in the unoriented part of the polymer specimen adjacent to the neck. The shear bands are oriented at an angle of about 45° with respect to the draw direction. When necking involves the unoriented part of the polymer, shear bands abruptly change their orientation and become aligned practically parallel to the draw axis.

DOI: 10.1134/S0965545X06050105

## INTRODUCTION

Mechanism of deformation of amorphous polymers in rubbery and glassy states has been the subject of ongoing research for many years [1–5]. A keen interest in this problem is due to at least two reasons. First, some aspects of deformation of amorphous polymers are not yet fully understood. Second, the wide practical use of amorphous polymers requires a deeper insight into their structural and mechanical behavior. An adequate description of a solid subjected to deformation necessitates the knowledge of structural rearrangements taking place on different scales. This problem has been successfully solved for semicrystalline polymers because the induced structural rearrangements can be observed at the level of crystallites [6]. In some cases, conformational rearrangements in macromolecules during their deformation can be studied using different methods, including IR spectroscopy or small-angle neutron scattering.

However, there is another scale of structural rearrangements in the deformed polymer, which is virtually unknown. These are structural rearrangements that are responsible for the distribution of stress fields and their evolution during deformation. A generally accepted concept is the assumption of affine deformation of rubbery polymers, which forms the basis for the statistical

theory of rubber elasticity [7]. However, even the first study performed with the use of this new procedure shows that this claim is far from being universal [8].

Another factor that must have an effect on the structural and mechanical behavior of deformed polymers is a change in surface area of test specimens. Although such a change is characteristic of deformation of any solid, this phenomenon is neither taken into account in any way nor studied. There are few reports on attempts to use direct microscopic methods for studying the mechanical characteristics of polymers. For example, Nishino et al. [9] determined the local values of Poisson's ratio for PET with atomic force microscopy and analyzed its dependence on the applied stress.

In some cases, e.g. for PET [10, 11], the polymer experiences stress-induced crystallization immediately during its stretching. Evidently, phase homogeneity in the polymer and, hence, the homogeneous character of stress field are disturbed in this case.

Recently [12–15], we have developed a direct microscopic examination procedure that allows this problem to be solved in many aspects. If a polymer specimen is decorated with a thin rigid coating prior to stretching (shrinkage), the subsequent deformation (shrinkage) of the specimen entails the formation of a certain pattern of relief in the coating and/or fragmentation of this coating. The mechanism of deformation (shrinkage) of the substrate polymer determines the character of surface structuring in the coating. Both

<sup>1</sup> This work was supported by the Russian Foundation for Basic Research, project nos. 03-03-32748 and 05-03-32538.

phenomena are fully governed by the specific features of transfer of mechanical stress from the substrate polymer to the coating across the interface. Relief formation in the coating is easy to study by direct microscopic observations, which provide information on the type and distribution of mechanical stresses in the deformed polymer. This microscopic procedure allowed us to explore the deformation of glassy polymers and to propose a new mechanism of their deformation that is based on direct microscopic examination of this process [12]. Moreover, this procedure also turned out to be effective in studying the deformation of amorphous polymers in the rubbery state. So far, this problem has not been a subject of close attention.

The objective of this study was to apply the direct microscopic procedure to the visualization of structural rearrangements that accompany the drawing of PET at temperatures above and below its glass transition temperature.

## EXPERIMENTAL

The samples studied were amorphous PET films of 100  $\mu\text{m}$  thickness. According to DSC data, the glass transition temperature of PET is 75°C. The test films were decorated with a thin (10 nm) platinum layer and then were stretched by 100% at different rates (from 0.2 to 1000 mm/min) at 90°C. After stretching, the samples with fixed dimensions were cooled to room temperature, and their surface was examined with a Hitachi S-520 scanning electron microscope. Some metal-decorated PET samples were stretched at room temperature with a draw rate of 10 mm/min. The stretching of the tests samples for further microscopic examination and characterization of stress-strain properties of the PET samples during their tensile drawing at a constant rate and under stress relaxation were carried out using an Instron 1122 universal tensile machine.

## RESULTS AND DISCUSSION

Figure 1 presents the SEM images of the platinum-decorated PET specimens after their 100% stretching at 90°C and different draw rates. In all cases, it is clearly seen that the surface layer of PET films underwent surface structuring (relief formation) in the metal coating during the deformation of the substrate polymer [16–18]. The main features of this deformation are the development of a wavy periodic relief and coating fracture into fragments of rather uniform size. The wavy relief is always oriented along the draw axis, whereas fracture cracks primarily propagate in the perpendicular direction.

An increase in the load rate imparts certain peculiar morphological features to the pattern of surface structuring. At low draw rates (0.2 and 2.0 mm/min), a fairly regular relief is formed. In this case, cracks propagate in the coating in a practically linear manner. As a result, the coating breaks down into ribbons with rather uni-

form dimensions, which span from one to the other side of the deformed specimens (Figs. 1a, 1b). At draw rates in the range of 20–200 mm/min (Figs. 1c, 1d), the relief is less regular. Some folds become inhomogeneous in both size and shape. Owing to the propagation of secondary cracks, which do not always reach the opposite side of the initial fragment, this fragment breaks down into smaller fragments; as a result, numerous branched fragments are formed on the polymer surface. Finally, at the maximum draw rate examined (1000 mm/min) (Fig. 1e), no long fractured coating fragments are observed any more. In this case, the coating breaks down via the formation of a continuous interpenetrating network with a variety of cracks that “connect” neighboring fragments. In the regions between these fragments, one can observe small isolated fragments of about 1  $\mu\text{m}$  size.

This finding suggests that the stress field induced in the polymer becomes progressively less homogeneous with an increase in the draw rate. Surface structuring patterns make it possible to visualize the disturbance of stress field homogeneity. At the same time, it is generally adopted that deformation is completely uniform (affine) if a polymer is deformed at temperatures above its glass transition temperature [7]. In the case of PET, which is capable of stress-induced crystallization, disturbance of phase homogeneity has been detected with the X-ray diffraction technique [10, 11]. In the absence of stress-induced crystallization, there is no cause of the disturbance of stress-field homogeneity during drawing. However, inhomogeneity is clearly revealed with the use of the proposed procedure.

Let us discuss the specific features of the deformation of polymer samples at high strain rates somewhat later. Now let us apply the analysis of surface structuring patterns in polymer samples with a thin rigid coating to the interpretation of the experimental results. Figure 2 presents  $\sigma$ - $\epsilon$  plots for the deformation of PET specimens by 100% at 90°C and different draw rates. It is clearly seen that the stress increases with an increase in the strain rate. As should be expected, this stress is proportional to the logarithm of strain rate.

According to the earlier speculations concerning the mechanism of surface structuring during the deformation of decorated polymers [16–18], the parameters of the formed microrelief are primarily determined by the mechanical stress. In particular, the wavelength  $\lambda$  of the formed regular relief (Eq. (1)) and the mean size  $L$  of fractured fragments (Eq. (2)) depend on the mechanical stress in the substrate polymer:

$$\lambda = 2h\sigma_y/\sigma_0, \quad (1)$$

$$L = 2h\sigma^*/\sigma_0, \quad (2)$$

where  $h$  is the thickness of the coating,  $\sigma_y$  is the yield stress of the coating,  $\sigma^*$  is the coating strength, and  $\sigma_0$  is the stress in the substrate.

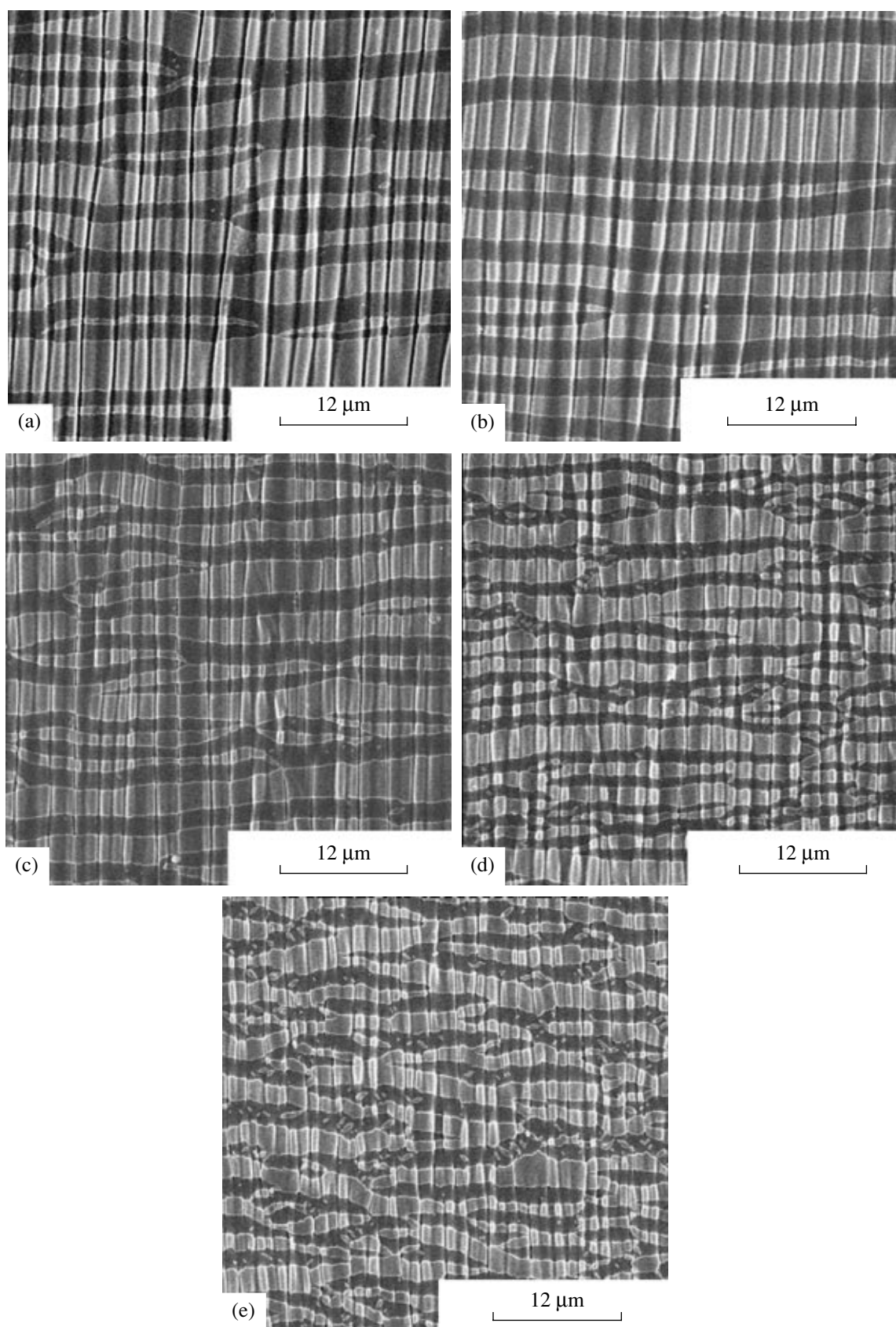


**Fig. 1.** Electron microphotographs of PET specimens decorated with a thin (10 nm) platinum layer after their stretching by 100% at 90°C and at draw rates of (a) 0.2, (b) 2.0, (c) 20, (d) 200, and (e) 1000 mm/min.

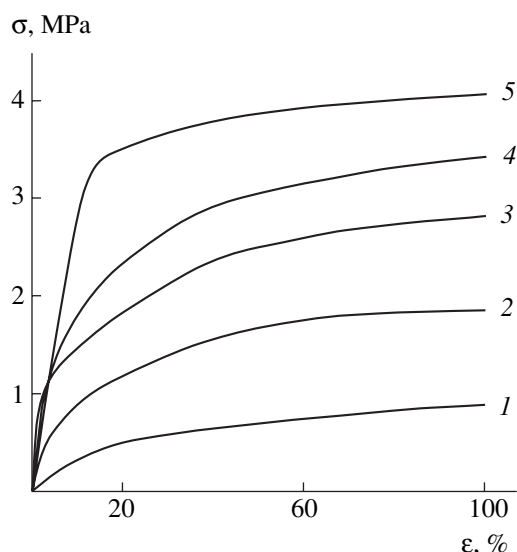


**Fig. 2.** Tensile stress–strain diagrams of platinum-decorated (10 nm) PET at 90°C and draw rates of (1) 0.2, (2) 2.0, (3) 20, (4) 200, and (5) 1000 mm/min.

As follows from Eqs. (1) and (2), both microrelief parameters  $\lambda$  and  $L$  should linearly decrease with an increase in the stress in the substrate or, which is the same, with an increase in the rate of drawing of the decorated polymer.

Figure 3 presents the wavelength of a formed regular microrelief plotted against the logarithmic draw rate. The values of  $\lambda$  decrease with an increase in the logarithm of draw rate, in agreement with our concept advanced earlier [17]. However, Fig. 3 shows a large scatter in the experimental data.

To understand the reasons behind this scatter, thorough control over the stress level in the test specimen is

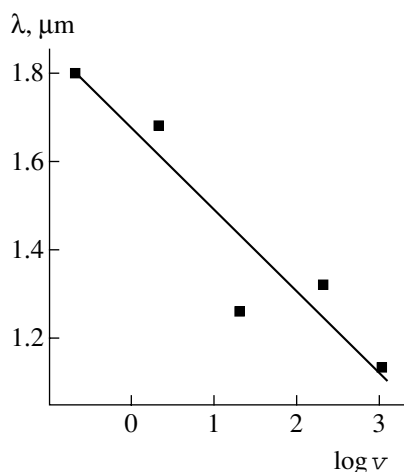


**Fig. 3.** Period  $\lambda$  of microrelief formed in platinum-decorated PET specimens stretched by 100% at 90°C vs. logarithm of strain rate.

required. Let us recall the procedure for the preparation of test samples for direct electron microscopic observations. After stretching, the samples with fixed dimensions were cooled to room temperature; then, their surface was studied with a scanning electron microscope. The cessation of drawing evidently leads to an immediate change in stress in the specimen subjected to deformation, since intense stress relaxation begins under such conditions.

Figure 4 illustrates this process at two different draw rates. After stopping the tensile testing device, the stress in the specimens begins to decrease violently. The most intense fall is observed immediately after stopping the draw, this process is most pronounced for the specimen deformed at the maximum draw rate.

As was shown earlier [19], the period of regular relief changes (increases) when PET specimens are held for different periods of time after their stretching at temperatures above the glass transition temperature. It was also shown that stress relaxation in the substrate led to structural rearrangement in the coating relief, so that new relief parameters corresponded to the level of time-dependent stress. Evidently, after stopping the tensile machine and during the subsequent cooling of the polymer to room temperature, the stress in the sample varies in an uncontrollable manner. Since all other parameters (temperature, draw ratio, thickness and nature of the coating) in the polymer were the same, it is this effect that is responsible, in our opinion, for the scatter in the experimental data in Fig. 3.

At the same time, the dependence of the mean size  $L$  of fracture fragments (Fig. 5) has a much lower scatter in experimental data and fits well with the behavior predicted by Eq. (2). This is due to the fact that disintegration (fragmentation) of the coating is irreversible in character, although it is determined by the stress level

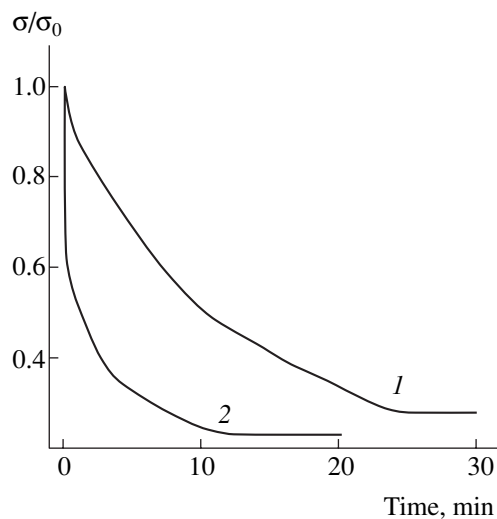


**Fig. 4.** Stress relaxation curves of the platinum-decorated PET specimens stretched by 100% at 90°C and draw rates of (1) 2 and (2) 200 mm/min.  $\sigma$  is the current stress and  $\sigma_0$  is the stress at  $\epsilon = 100\%$ .

in the substrate; as a consequence, the mean dimensions of fracture fragments cannot change under the stress relaxation conditions in the polymeric substrate.

Let us turn back to the analysis of structural and mechanical behavior of the PET specimen deformed at the maximum draw rate (Fig. 1e). As has been mentioned above, this specimen has a number of specific morphological features that differentiate it from the specimens deformed at slower draw rates. Note one interesting feature of the PET deformed at temperatures above its  $T_g$ . It is well known [10, 11] that PET is capable of strain-induced crystallization at rather high draw rates. The drawing of PET at relatively low rates in the range 80–100°C gives rise only to molecular orientation, while leaving the polymer as a whole in the amorphous state. At fast draw rates in this temperature range, an oriented crystalline structure is formed in the polymer. The development of the crystalline structure in the deformed polymer naturally leads to its structural inhomogeneity and, hence, to additional perturbation of the field homogeneity of acting stresses.

The question arises as to whether the strain-induced crystallization of PET can be visualized with the use of the procedure in question. To answer this question, we performed the following experiment. A PET specimen was deformed by 100% at 90°C and a draw rate of 1000 mm/min and then cooled in the grips of the testing machine. Next, the specimen was decorated with a thin (10 nm) platinum layer and annealed at 100°C. As a result of this thermal treatment, the polymer experienced shrinkage, and the applied coating made it possible to visualize the structural rearrangements induced under these conditions. An analysis of structural rearrangements during the shrinkage of the polymer allows many other features of its deformation to be revealed. Note that strain-induced crystallization indeed takes place in PET at high draw rates (1000 mm/min). In particular, this conclusion is confirmed by the low values of shrinkage at 100°C. The polymer specimen deformed at a fast draw rate exhibits as low a shrinkage as 22% by annealing. At the same time, the PET specimen stretched by 100% at 90°C and a strain rate of 2 mm/min shows practically complete shrinkage (95%) under the same annealing conditions. However, the shrinkage to even such a low extent of the PET sample deformed at a high draw rate allowed us to reveal interesting structural features of its reversible deformation.

Figure 6 presents an SEM image of the PET specimen subjected to tensile drawing by 100% at 90°C and a rate of 1000 mm/min and to temperature-stimulated shrinkage under the above conditions. As is seen at high magnifications (Fig. 6a), polymer shrinkage leads to similar morphological changes in the surface layer, as in the case of “direct” drawing. Indeed, as a result of shrinkage, the coating acquires a certain wavy relief, although not as regular as that after direct drawing.

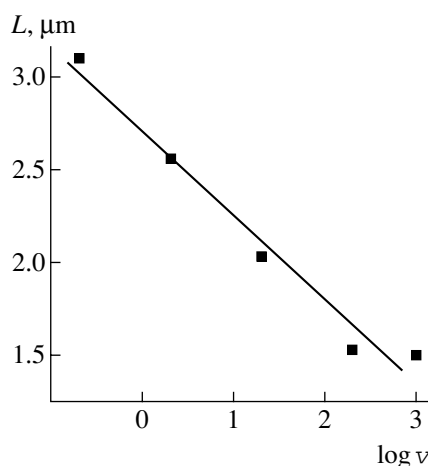


**Fig. 5.** Average size of fracture fragments versus the logarithm of draw rate for the platinum-decorated PET specimens stretched by 100% at 90°C.

At the same time, for the PET specimen stretched at a high rate above its glass transition temperature, we managed by means of the new procedure to reveal certain specific morphological features other than those observed for PET specimens subjected to direct drawing at lower draw rates. As follows from Fig. 6b, straight bands crossing the sample and each other at different angles appear on the surface of the sample.

This pattern resembles the system of shear bands that is formed during annealing of amorphous polymers oriented below  $T_g$  [13, 14]. For comparison, Fig. 7 presents the AFM image of the PET specimen deformed in the uniaxial compression mode and annealed at 100°C (prior to annealing, this specimen was decorated with a thin metal layer). It is clearly seen that these bands are grooves, into which the metal coating is drawn. The range of these phenomena and their interpretation are detailed in [13, 14]. A close inspection of the straight morphological entities that emerge during the shrinkage of PET samples stretched at high draw rates above the glass transition temperature (Fig. 6) allows one to notice their essential morphological features. It turns out that these bands are not grooves on the surface of the decorated polymer. As follows from Fig. 6c, they constitute small cracks aligned in a certain direction that is dictated by the polymer matrix. This result suggests that the processes responsible for the shrinkage of the polymer deformed at high draw rates above (Fig. 6) and below the glass transition temperature (Fig. 7) have different mechanisms. It is hardly possible to arrive at this conclusion using other investigation techniques. At present, it is difficult to explain the origin of the morphological entities revealed during the shrinkage of the polymer deformed at a high draw rate. Nonetheless, it may be stated that the shrinkage of PET deformed at a fast draw rate above its glass transition temperature proceeds in a rather nonuniform manner, thus indicating inhomogeneity of the polymer structure, a property

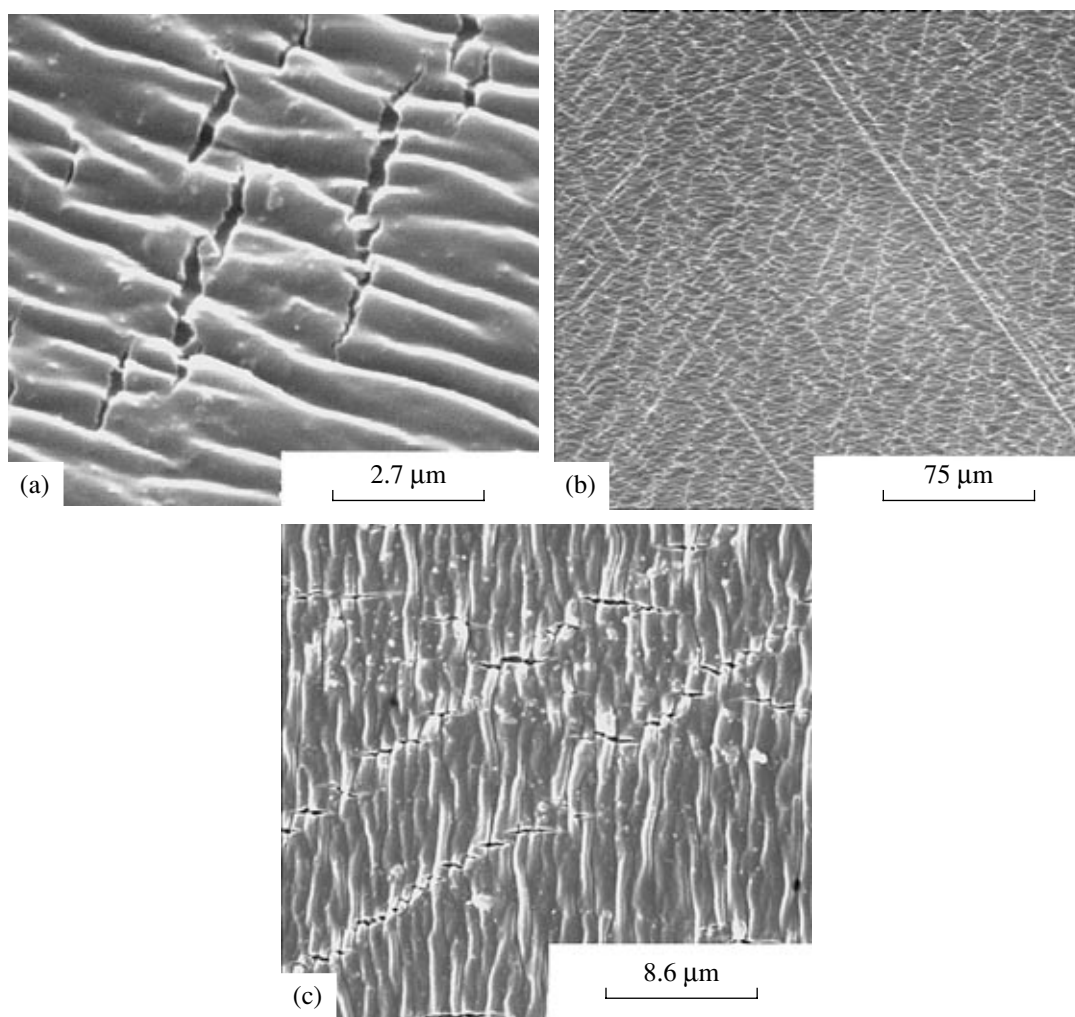


**Fig. 6.** Electron microphotographs of the PET specimen after its stretching by 100% at 90°C and at a draw rate of 1000 mm/min (at different magnifications). After drawing, the deformed sample was decorated with a thin (10 nm) platinum coating and annealed at 100°C. See the text for details.

that disturbs the uniformity of the stress field responsible for this process.

The question now arises whether this microscopic procedure is useful for revealing inhomogeneous plastic deformation in PET directly during its stretching at temperatures below the glass transition temperature. To study this problem, the following experiment was performed. PET specimens decorated with a thin (10 nm) platinum layer were deformed at room temperature via necking. As was shown in [20], coating fragmentation takes place in the narrow transition region between the unoriented part of the polymer and the propagating neck in this case. Figure 8a presents a microphotograph of the polymer region located at the boundary between the neck and unoriented part of the sample. One can see that the thickness of the sample dramatically decreases in this region; as a result, its initial smooth surface noticeably bends, and this bending is evidently accompanied by cracking of the coating. This procedure also

makes it possible to visualize the development of shear bands in this region. It is clearly seen that these shear bands propagate through this transition region linearly at an angle of 45° with respect to the direction of tensile drawing.

It is well known that the transition layer between the unoriented part of the polymer and the propagating neck drifts, with an increase in strain, along the sample until its complete transformation into a neck. Fragmentation of the coating is primarily localized in the region of orientational drawing of polymer, an area that is adjacent to the above transition layer [20]. Figure 8b shows a part of the specimen that contains a fragment of the transition layer, as well as a part of the necked specimen. It is distinctly seen that the shear bands that have appeared in the transition layer reach the necked region. Since the necking of PET takes place at a much higher stress than drawing above its  $T_g$  (Fig. 1), the coating breaks down into much smaller fragments

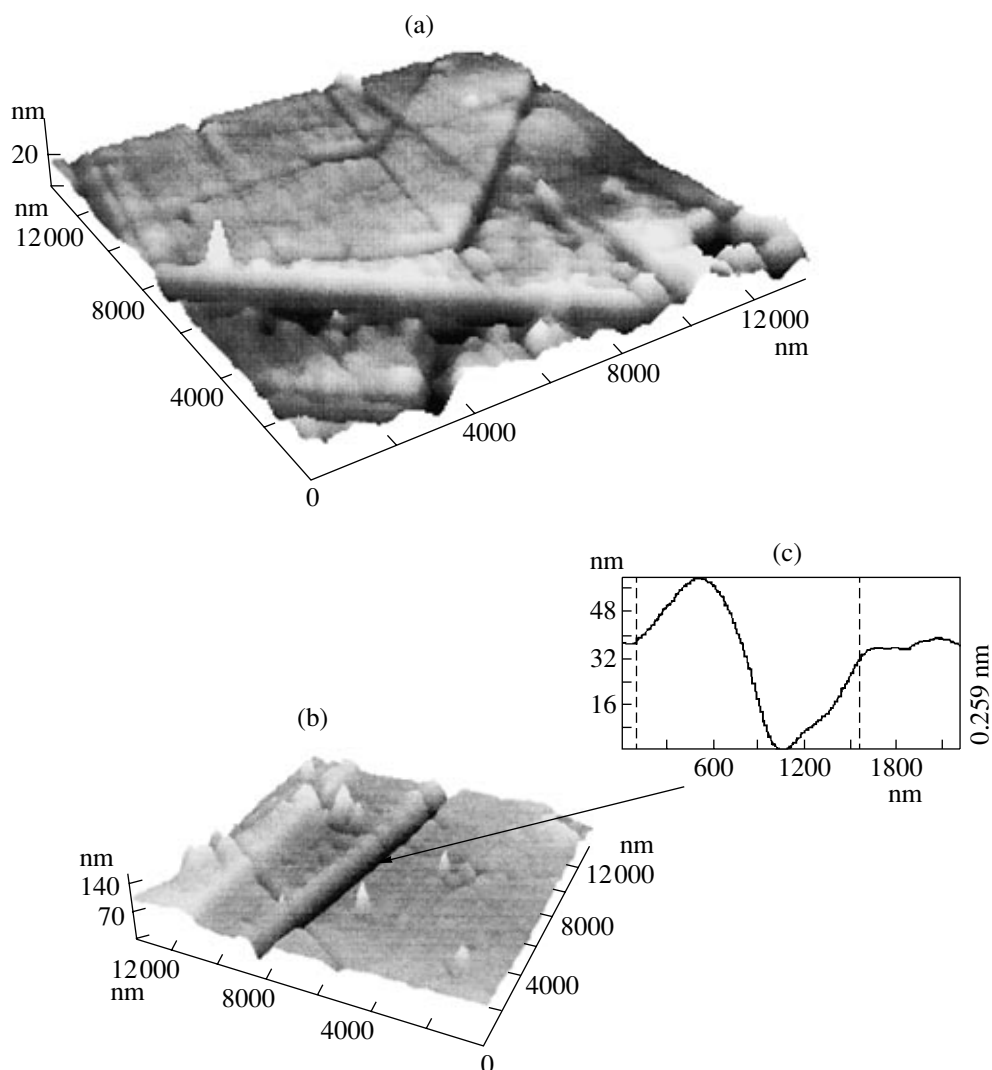


**Fig. 7** Three-dimensional reconstruction of the AFM image of surface of the PET specimen deformed in the plane compression mode. After decoration with a thin (10 nm) platinum layer, the sample experienced an 18% plane shrinkage during annealing. (a)  $10 \times 10 \mu\text{m}$ ; (b) image of a single shear band; (c) profilogram of the shear band.

(Fig. 8b). Nevertheless, in the regions where shear bands extend to the neck area, the coating experiences additional fragmentation which leaves a distinct trace on its surface. This localized fragmentation allows one to follow further evolution of shear bands. It turns out that these shear bands lose their  $45^\circ$  orientation with respect to the draw direction when coming into the neck area. They become aligned with the draw axis and are involved in the neck structure. The shear bands involved in the neck are clearly seen in areas at any distance from the polymer necking onset region (Fig. 8c). Of course, once shear bands become included into the neck structure, they cannot be further referred to as “shear bands.” The point is that the shear bands formed by the deformation of unoriented polymer are composed of oriented fibrillar material [21]. During further deformation, the polymer containing shear bands is

involved in the structure of the propagating neck. As follows from the data presented above, the structure of the neck formed is not homogeneous. The neck material “remembers” that the transition into oriented state is performed by the polymer containing shear bands. If the neck in PET is subjected to shrinkage, for example, with a swelling solvent, a system of shear bands will appear in the resultant material, which is easy to detect with a light microscope [22].

The obtained data support our earlier conclusion that a glassy polymer after its plastic deformation has a complex structure [23] composed of at least two components. One component is the material localized in shear bands that are involved in the neck and have a specific highly dispersed fibrillar structure [21]. The other is the main portion of the oriented polymer without well-defined interfaces, which serves as a matrix

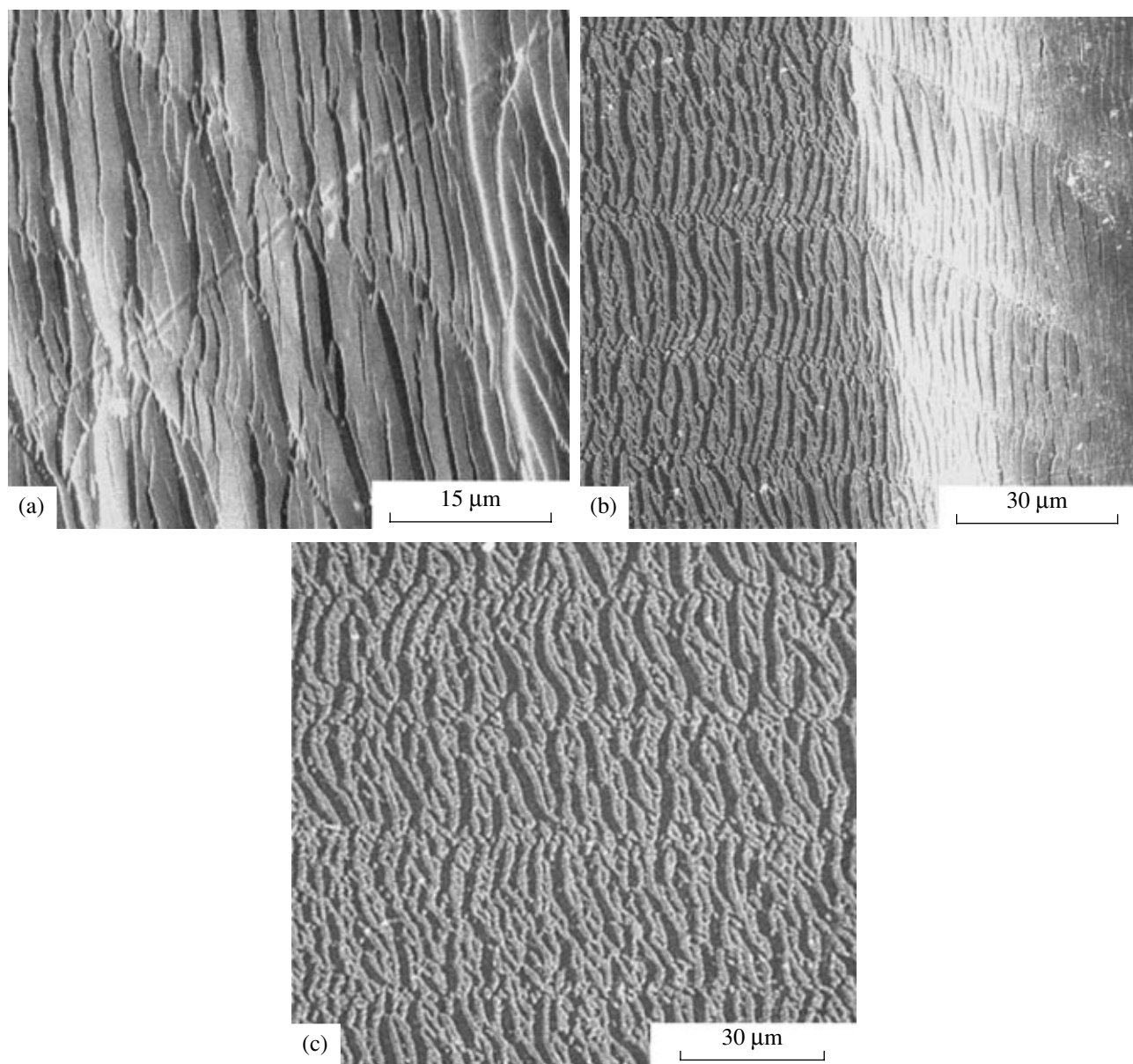


**Fig. 8.** Electron microphotographs of the platinum-decorated (10 nm) PET specimen stretched at room temperature to necking: (a) transition region where polymer is transformed into a neck, (b) a part of the specimen in the transition layer (right) coexisting with a fragment of the formed neck (left), and (c) a remote area of the formed neck at a distance from the transition layer.

that incorporates the zones having the highly dispersed fibrillar structure formed in shear bands. As is seen, the direct electron microscopic procedure makes it possible to visualize various earlier unknown structural rearrangements that accompany large strains in amorphous polymers.

Thus, the presented experimental results demonstrate the efficacy of the microscopic examination procedure used for studying strain-induced structural rearrangements in amorphous polymers. It may be expected that this procedure will be instrumental in obtaining new structural data concerning the mecha-

nism of polymer deformation at temperatures above and below its glass transition temperature.

#### REFERENCES

1. Yu. S. Lazurkin, Doctoral Dissertation in Mathematics and Physics (Moscow, 1954) [in Russian].
2. *Structural and Mechanical Behavior of Glassy Polymers*, Ed. by M. S. Arzhakov, S. A. Arzhakov, and G. E. Zaikov (Nova Science, New York, 1997).
3. E. F. Oleynik, *High Performance Polymers*, Ed. by E. Baer and S. Moet (Hanser, Berlin, 1991), p. 79.

4. *The Physics of Glassy Polymers*, Ed. by R. N. Haward and B. Y. Young (Chapman & Hall, London, 1997).
5. S. V. Shenogin, G. W. H. Hohne, O. B. Salamatina, et al., *Vysokomol. Soedin.*, Ser. A **46**, 30 (2004) [*Polymer Science*, Ser. A **46**, 21 (2004)].
6. E. F. Oleinik, *Vysokomol. Soedin.*, Ser. C **45**, 2137 (2003) [*Polymer Science*, Ser. C **45**, 17 (2003)].
7. L. Treloar, *The Physics of Rubber Elasticity* (Oxford Univ. Press, Oxford, 1949; Inostrannaya Literatura, Moscow, 1953).
8. A. L. Volynskii, T. E. Grokhovskaya, A. V. Bol'shakova, et al., *Vysokomol. Soedin.*, Ser. A **46**, 1332 (2004) [*Polymer Science*, Ser. A **46**, 806 (2004)].
9. T. Nishino, A. Nozawa, M. Kotera, and K. Nakamae, *Rev. Sci. Instrum.* **71**, 2094 (2000).
10. P. G. Llana and M. C. Boyce, *Polymer* **40**, 6729 (1999).
11. A. Mahendrasingam, C. Martin, W. Fuller, et al., *Polymer* **40**, 5553 (1999).
12. A. L. Volynskii, T. E. Grokhovskaya, A. S. Keчек'yan, et al., *Dokl. Akad. Nauk* **374**, 644 (2000).
13. A. L. Volynskii, A. S. Keчек'yan, T. E. Grokhovskaya, et al., *Vysokomol. Soedin.*, Ser. A **44**, 615 (2002) [*Polymer Science*, Ser. A **44**, 374 (2002)].
14. A. L. Volynskii, T. E. Grokhovskaya, A. S. Keчек'yan, and N. F. Bakeev, *Vysokomol. Soedin.*, Ser. A **45**, 449 (2003) [*Polymer Science*, Ser. A **45**, 265 (2003)].
15. A. L. Volynskii, T. E. Grokhovskaya, V. V. Lyulevich, et al., *Vysokomol. Soedin.*, Ser. A **46**, 247 (2004) [*Polymer Science*, Ser. A **46**, 130 (2004)].
16. A. L. Volynskii, S. L. Bazhenov, O. V. Lebedeva, et al., *J. Appl. Polym. Sci.* **72**, 1267 (1999).
17. A. L. Volynskii, S. L. Bazhenov, O. V. Lebedeva, and N. F. Bakeev, *J. Mater. Sci.* **35**, 547 (2000).
18. S. L. Bazhenov, A. L. Volynskii, V. M. Alexandrov, and N. F. Bakeev, *J. Polym. Sci.*, Part B: Polym. Phys. **40**, 10 (2002).
19. A. L. Volynskii, E. E. Voronina, S. L. Bazhenov, and N. F. Bakeev, *Dokl. Akad. Nauk* **363**, 638 (1998).
20. L. M. Yarysheva, D. A. Panchuk, S. V. Moiseeva, et al., *Vysokomol. Soedin.*, Ser. A [*Polymer Science*, Ser. A] (in press).
21. J. C. M. Li, *Polym. Eng. Sci.* **24**, 750 (1984).
22. A. S. Keчек'yan, *Vysokomol. Soedin.*, Ser. B **29**, 804 (1987).
23. A. L. Volynskii and N. F. Bakeev, *Vysokomol. Soedin.*, Ser. C **47**, 1332 (2005) [*Polymer Science*, Ser. C **47**, 74 (2005)].